Site Determination and Thermally Assisted Tunneling in Homogenous Nucleation

Jascha Repp,[1,2] Gerhard Meyer,[1,2] Karl-Heinz Rieder,[2] and Per Hyldgaard[3]

[1]*IBM Research, Zurich Research Laboratory, CH-8803 Rüschlikon, Switzerland*

[2]*Institut für Experimentalphysik, Freie Universität Berlin, Arnimallee 14, D-14195 Berlin, Germany*

[3]*Department of Applied Physics, Chalmers University of Technology and Göteborgs University, S-41296, Göteborg, Sweden*

(Received 21 March 2003; revised manuscript received 16 July 2003; published 12 November 2003)

A combined low-temperature scanning tunneling microscopy and density functional theory study on the binding and diffusion of copper monomers, dimers, and trimers adsorbed on Cu(111) is presented. Whereas atoms in trimers are found in fcc sites only, monomers as well as atoms in dimers can occupy the fcc as well as the metastable hcp site. In fact the dimer fcc-hcp configuration is only 1.3 meV less favorable with respect to the fcc-fcc configuration. This enables a confined intracell dimer motion, which at temperatures below 5 K is dominated by thermally assisted tunneling.

DOI: 10.1103/PhysRevLett.91.206102 PACS numbers: 68.35.Fx, 68.37.–d, 68.55.–a

In recent years important progress has been made in understanding epitaxial growth processes on the atomic scale, from both the experimental and the theoretical side. Early experiments employed field ion microscopy (FIM), whereas in recent years scanning tunneling microscopy (STM) proved to be a perfect technique for this task.

Interestingly, the first steps in the homoepitaxial growth on fcc (111) noble-metal surfaces still belong to the unsolved problems. Compared to the more open metal surfaces, the behavior of single adatoms is more complicated on (111) surfaces, because adatoms can reside in two different binding sites, the so-called fcc and hcp sites. Whereas the fcc site continues the *ABC* layer stacking of the bulk the hcp site breaks this sequence. As the energy difference between the two sites can be very small, the site occupation preference is expected to depend critically on the size of the metal structures, as was demonstrated experimentally for Ir/Ir(111) [1,2].

The experimental determination of the fcc/hcp site preference of individual adatoms is a difficult task, and only two experimental studies exist. Wang and Ehrlich determined single adatoms of Ir/Ir(111) to be located on hcp sites [3,4], whereas in the case of Pt/Pt(111) a clear fcc site preference was found [5]. A rule predicting the site preference was later developed for metals having a partly filled *d* band [6,7]. Whereas no experimental work can be found in the literature for systems without a partly filled *d* shell, several theoretical studies exist. First-principles theoretical work by Stumpf and Scheffler [8] and Feibelman [9] predicted an hcp site preference for individual Al atoms on Al(111). Other theoretical studies on copper, silver, and gold do not find any clear hcp or fcc site preference for a single adatom [10,11]. Clearly, very subtle contributions of both the electronic structure and the local relaxation have to be taken into account [12], and therefore no general rule is available to predict the preferred binding site.

In this work we determined the adsorption site of Cu metal adatoms to be the fcc site, by means of a unique technique of STM diffusion studies in combination with atomic manipulation, applicable also for systems that cannot be studied by FIM. Moreover a particular localized diffusion behavior of Cu dimers has been observed experimentally, with the properties as predicted earlier in a theoretical work by Bogicevic *et al.* [13]. Despite the large mass of Cu atoms, this localized diffusion is dominated below 5 K by thermally assisted tunneling of Cu adatoms. Copper as a noble metal is characterized by an almost complete *d*-band occupation, making the existing, qualitative theoretical analysis of site preference [6,7] indeterminate. Instead the experimental results are complemented by an extensive set of large-scale *ab initio* density functional theory (DFT) calculations.

Our experiments were performed with a low-temperature STM operated at 4–21 K. The sample was cleaned by sputtering and annealing cycles. Bias voltages refer to the sample voltage with respect to the tip. To measure possible tip effects we determined the hopping rate for different tunneling parameters and varied the tip-adatom interaction time by taking an image series for different time intervals. Using atomic manipulation the atoms were positioned far away from defect sites. The measured temperatures were calibrated within 0.1 K.

Our calculations are within the generalized gradient approximation (GGA) using the plane-wave ultrasoft-pseudopotential code DACAPO [14]. We used slab supercell geometries with a vacuum separation $\gtrsim$13 Å, and with a five- (four-)layer slab thickness and a 3-by-3 (4-by-5) atom insurface extension to map the monomer (dimer) adsorption and dynamics. The two lowermost layers were kept frozen in a bulk-lattice structure. The adsorbates and surface atoms were relaxed to 0.05 eV/Å using an energy cutoff of 30 Ry, with dipole correction enabled. Our DFT calculations should determine the local relaxation, binding, and vibrations extremely accurately. However, *ab initio* DFT can encounter difficulties in resolving the energy variation between different adsorption sites if they are in the range of only a few meV [15].

Consequently, we have tested the robustness of our results and used a carefully controlled sampling of k points: a standard choice of 2×2 with a 0.1 eV Fermi smearing tested against 4×4 k-point calculations with a 0.025 eV smearing. In addition, we have tested the monomer site-preference result against calculations using a fully relaxed four-layer 5-by-4 unit cell.

The diffusion paths of individual adatoms were mapped by taking a series of consecutive STM images on Cu/Cu(111). Five series of more than 100 images each were taken at different temperatures between 11 and 12 K, allowing the determination of the diffusion barrier as $E_B = (37 \pm 5)$ meV [16], in good agreement with other experiments [17,18] as well as theory [10,19]. The mapping of the relative movement of one adatom in between subsequent images clearly reveals the hexagonal lattice of the substrate surface, showing that only one adsorption site is observed. As pointed out by Wang and Ehrlich [4], the conventional technique of mapping diffusion paths is not applicable for a site determination if only one of the sites is occupied. On the other hand, lateral manipulation on the atomic scale [20,21] can in general be used as a tool to access also metastable sites by artificial occupation of nonequilibrium configurations [22].

For this type of extension of the mapping technique, individual adatoms were repeatedly repositioned using lateral manipulation at a temperature of 7 K. At this temperature the monomers can be positioned in both the fcc and the hcp sites, making the site determination possible. If the temperature is increased to $\simeq$10 K the individual adatoms regain their equilibrium position, which can now be identified as the fcc site (see Fig. 1).

In order to have a point of origin for this extended site-mapping technique, the positions were determined with respect to a monatomic copper row built up atom by atom. The row ran parallel to one of the close-packed $[1\bar{1}0]$ directions. The lateral distances between the individual adatoms and the row were $|\Delta x| = n\sqrt{3/8}a_0$, with integer values of n for the fcc positions and fractional values of n for the hcp positions. In addition, this shows that the atoms in the row reside in fcc positions in agreement with our theoretical calculations [23].

The diffusion experiments, in which no hcp-monomer occupation could be identified, revealed that the hcp-to-fcc hopping rate is at least 75 times higher than the fcc-to-hcp hopping rate, providing a lower bound for the energy difference of the two sites of $|\Delta E| \geq kT \ln(75) =$ 4 meV. Alternatively, the hopping from hcp to fcc sites, which sets in at a temperature that is $\Delta T \simeq 1.5$ K lower than the onset for fcc-to-hcp hopping, allows a rough estimate of the energy difference for the two sites as $\Delta E \simeq E_B \Delta T/T$. Taking the experimental uncertainties into account, this provides an upper bound of $\Delta E \leq$ 8 meV, subject to the assumption that the fcc and hcp diffusion prefactors differ by no more than a factor of 10 (in fact our theory calculations yield identical prefactors of $\nu_0 = 1 \times 10^{12}$ s^{-1} [24]).

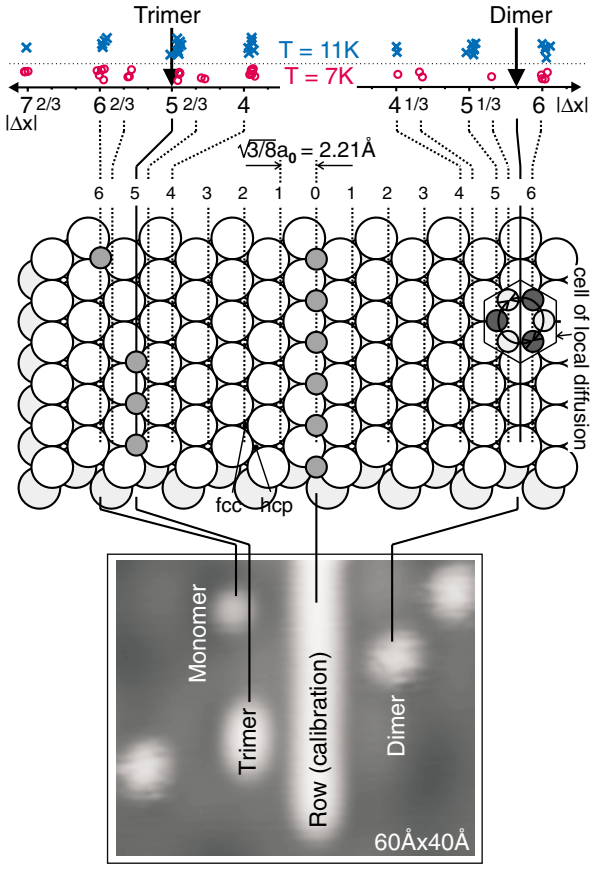

FIG. 1 (color online). By means of an extended site-mapping technique the adsorption site of Cu/Cu(111) was determined to be the fcc site. Individual adatoms were repeatedly repositioned using lateral manipulation at a temperature of 7 and 11 K. One STM image of a series and the corresponding model are shown. In the topmost part of the figure, the positions of these individual adatoms (circles at 7 K, crosses at 11 K) as well as of a dimer and a trimer (arrows) with respect to the row are shown.

This result is consistent with a previous DFT study [25] and congruent with our DFT calculations that yield an fcc preference of about 6 meV. An identical energy difference of 6 meV arises in a corresponding DFT study of monomer adsorption on a prerelaxed frozen surface, or when we increase the k-point sampling while lowering the smearing. A similar fcc preference arises when, instead, we use a four-layer 5-by-4 unit cell. These tests [25] suggest that the monomer calculations are converged with respect to the choice of DFT parameters. The small monomer-adsorption preference reflects subtle differences in the interplay between the adsorbate-induced density response and the exact location of subsurface atoms, as we shall discuss further in a forthcoming publication.

In experiments, dimers do not exhibit any translational diffusion up to a temperature of 21 K. Nonetheless they already diffuse locally at a temperature as low as 7 K, as can be seen from the unstable appearance of the dimer in the STM image shown in Fig. 2(a). As predicted by

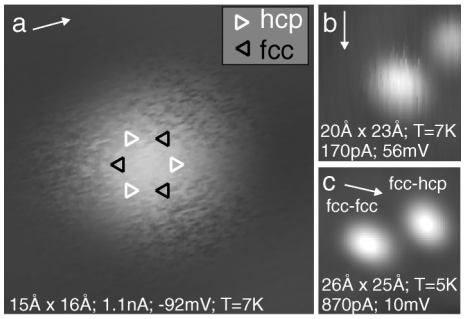

FIG. 2. (a) At $T = 7$ K Cu dimers appear unstable in STM images, showing that local diffusion takes place during scanning. (b) Long-range interactions with a monomer close by can stabilize the dimer. (c) At a temperature of 5 K, the dimer diffusion is slow enough to trace individual diffusion steps. The white arrows indicate the fast scan direction. The crystal orientation corresponds to the one in Fig. 1.

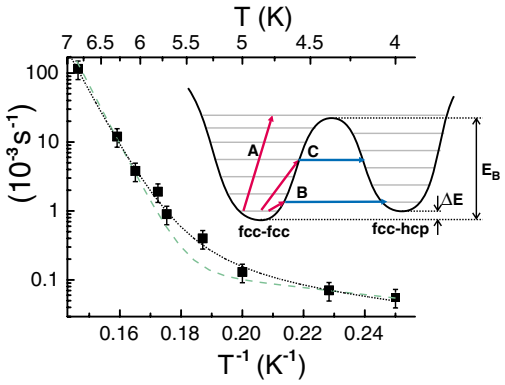

FIG. 3 (color online). Arrhenius plot of the dimer ff to fh hopping rate. The hopping rate is determined by direct thermal activation (process A) at temperatures above 6 K and by thermally assisted tunneling to the ground state (process B) below 5 K. The dashed line represents a fit, taking only these two processes into account. At $4.5 \leq T \leq 6$ K an even better fit (dotted line) is obtained by including also thermally assisted tunneling for all intermediate energies (process C). Scanning at $U = 10$ mV, $I = 10$ pA excluded tip-induced diffusion.

theory [13] and verified by the site determination demonstrated in Fig. 1, the local diffusion takes place in a cell centered around one atom in the topmost layer of the substrate surface. This cell of local diffusion consists of three hcp and three fcc sites around the on-top position of the substrate atom (see scheme in Fig. 1). In the following we will use the notation ff, hh, fh, fb, hb, and bb for fcc-fcc, hcp-hcp, fcc-hcp, fcc-bridge, hcp-bridge, and bridge-bridge dimer occupations, respectively.

As can be seen in Fig. 2(b) a dimer can be stabilized by long-range interactions [16,26,27] with another monomer positioned close to the dimer. Moreover, reducing the temperature to below 7 K, the dimer intracell diffusion becomes so slow that it is possible to trace the individual diffusion steps by recording a series of STM images. The stable ff and the metastable fh configuration can be observed [see Fig. 2(c)]. The relative probability of observation at 5 K ($P_{\mathrm{fh}}/P_{\mathrm{ff}} \simeq 1/20$) yields an energy difference of only $\Delta E = -kT \ln(P_{\mathrm{fh}}/P_{\mathrm{ff}}) = (1.3 \pm 0.5)$ meV. The hh configuration could not be found.

An Arrhenius plot of the dimer ff to fh hopping rate (Fig. 3) documents that thermally assisted tunneling [22,28,29] enables the hopping of the dimers at very low temperatures ($T \leq 5$ K), despite the large mass m_{Cu} of a Cu atom. In a simple model with a parabolic barrier at the transition state fb, characterized by an imaginary frequency ω_{fb} through $E = E_B + \frac{1}{2}(m_{\mathrm{Cu}}\omega_{\mathrm{fb}}^2 x^2)$, the transmission probability due to tunneling for an energy ϵ is known to be approximately $\exp[-2i\pi(E_B - \epsilon)/\hbar\omega_{\mathrm{fb}}]$ [30]. In the case of thermally assisted tunneling this probability has to be multiplied by the probability for thermal activation to the energy ϵ of $\exp(-\epsilon/kT)$. This results in a critical temperature $T_C = \hbar\omega_{\mathrm{fb}}/2i\pi k$, which marks the limit between thermally activated hopping and thermally assisted tunneling. Above this temperature we obtain the conventional Arrhenius behavior with the activation energy E_B, whereas for the low-temperature regime, only thermally assisted tunneling to the ground state is relevant, and the slope in the Arrhenius plot is determined by the energy difference ΔE of the two ground states. Only in the temperature region just below T_C do all intermediate processes come into play (see fits in Fig. 3). The fit to the data yields $\nu_0 = 8 \times 10^{11 \pm 0.5}\ \mathrm{s}^{-1}$ and $E_B = 18 \pm 3$ meV. Assuming the barrier to be cosine shaped, ω_{fb} and thus T_C can be estimated from the distance $d = 1.47$ Å between the fcc and the hcp sites and the barrier height E_B as $T_C \simeq \sqrt{E_B/2m_{\mathrm{Cu}}}\hbar/kd = 6.0$ K, in agreement with experiment. The surprising observation of the tunneling of a heavy Cu atom can be understood when considering that the atom not only has a very low barrier but also an exceptionally small distance to overcome. In contrast to the recently reported tunneling of carbon adatoms [22], we do not see any influence of discrete vibrational levels of the dimer. This indicates a very strong vibronic coupling of the dimer to the substrate, clearly ruling out the possibility of a $Cu_2/Cu(111)$ quantum rotor [13].

From calculations using 2×2 k-point sampling (Fig. 4, dashed lines), we predict an intracell dimer-energy variation that is in qualitative agreement with the original

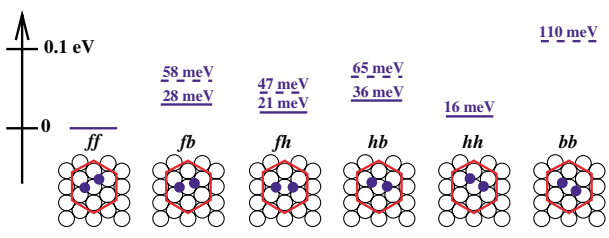

FIG. 4 (color online). Illustration of the DFT analysis of the dimer intracell dynamics [13] observed on Cu(111). Solid (dashed) lines illustrate the variation in the fully relaxed dimer-configuration energies calculated using the 4×4 (2×2) k-point sampling.

TABLE I. Site preferences, kinetic barriers, and stability of monomers, dimers, and trimers on Cu(111) as observed in low-temperature STM and calculated in first-principles DFT.

	STM	DFT
Monomer: preferred site	fcc	fcc
diffusion barrier E_B (meV)	37 ± 5	50
attempt frequency ν_0 (s^{-1})	$5 \times 10^{13\pm1}$	1×10^{12}
$\Delta E = E_{\text{hcp}} - E_{\text{fcc}}$ (meV)	$4 \leq \Delta E \leq 8$	6
Dimer: preferred site	fcc-fcc	fcc-fcc
intracell-diffusion E_B (meV)	18 ± 3	28
$E_{\text{fcc-hcp}} - E_{\text{fcc-fcc}}$ (meV)	1.3 ± 0.5	21
Trimer/row: preferred site	fcc	fcc

Al-dimer study [13]. As in these previous theoretical calculations and consistent with the experiments, we find that intracell rotation remains possible even when low temperatures inhibit the net intercell diffusion, for which we determine a concerted-sliding barrier $E_{B,\text{dif}} \approx 190$ meV. Using the more accurate 4×4 k-point sampling we predict an energy variation (Fig. 4, solid lines), in even better agreement with experimental observations. The 4×4 k-point calculations establish a near degeneracy between the ff, fh, and hh dimer configurations and a significantly reduced effective rotation barrier, i.e., the energy of the fb configuration. The accuracy improvement obtained by using the 4×4 k-point sampling in the dimer-configuration survey is selective and correlated with the dimer-induced surface distortion as also previously found in the Al ad-dimer study [13]. We attribute the experimental observation of dimer confinement to the rotation process, ff $\rightarrow$ fb $\rightarrow$ fh (and back), which has a lower barrier than the ff $\rightarrow$ fb $\rightarrow$ fh $\rightarrow$ hb $\rightarrow$ hh rotation and the direct ff $\rightarrow$ bb $\rightarrow$ hh transition.

Trimers were found to be always of a fcc-fcc-fcc type and stable in the temperature range of 5–21 K.

In summary, we have shown that individual copper adatoms as well as adatoms in dimers, trimers, and larger structures prefer fcc over hcp sites on Cu(111). The experimentally observed difference in binding energy for the monomer is only about 6 meV. Moreover, in the case of copper dimers, we were able to observe a confined intracell metal dimer motion for a wide temperature range of 4–21 K, which at low temperatures is enabled by thermally assisted tunneling. Even though the small energy differences inherent in this system may attain the limits of current DFT accuracy, a detailed DFT analysis yields monomer and dimer energetics that are in very good agreement with the experiments (see Table I).

We thank Professor G. Ehrlich and Professor M. Scheffler for their very valuable comments and acknowledge partial funding by the EU TMR project "AMMIST," the EU IST-FET project "NICE," the Deutsche Forschungsgemeinschaft Project No. RI 472/3-2, the Chalmers UNICC (for supercomputing), and the Swedish Foundation for Strategic Research via ATOMICS (P. H.).

[1] S. C. Wang and G. Ehrlich, Surf. Sci. **239**, 301 (1990).
[2] C. Busse *et al.*, Phys. Rev. Lett. **91**, 056103 (2003).
[3] S. C. Wang and G. Ehrlich, Phys. Rev. Lett. **62**, 2297 (1989); Surf. Sci. **224**, L997 (1989).
[4] S. C. Wang and G. Ehrlich, Surf. Sci. **246**, 37 (1991); Phys. Rev. Lett. **68**, 1160 (1992).
[5] A. Gölzhäuser and G. Ehrlich, Phys. Rev. Lett. **77**, 1334 (1996).
[6] B. Piveteau, D. Spanjaard, and M. C. Desjonquères, Phys. Rev. B **46**, 7121 (1992).
[7] S. Papadia, B. Piveteau, D. Spanjaard, and M. C. Desjonquères, Phys. Rev. B **54**, 14 720 (1996).
[8] R. Stumpf and M. Scheffler, Phys. Rev. Lett. **72**, 254 (1994); Phys. Rev. B **53**, 4958 (1996).
[9] P. J. Feibelman, Phys. Rev. Lett. **69**, 1568 (1992).
[10] U. Kürpick, Phys. Rev. B **64**, 075418 (2001).
[11] G. Boisvert, L. J. Lewis, M. J. Puska, and R. M. Nieminen, Phys. Rev. B **52**, 9078 (1995).
[12] M. Giesen and H. Ibach, Surf. Sci. **529**, 135 (2003).
[13] A. Bogicevic, P. Hyldgaard, G. Wahnström, and B. I. Lundqvist, Phys. Rev. Lett. **81**, 172 (1998).
[14] DACAPO (http://www.fysik.dtu.dk/CAMPOS) version 1.30 with extensions by L. Bengtsson using GGA(PW91).
[15] P. J. Feibelman *et al.*, J. Phys. Chem. B **105**, 4018 (2001).
[16] J. Repp *et al.*, Phys. Rev. Lett. **85**, 2981 (2000).
[17] N. Knorr *et al.*, Phys. Rev. B **65**, 115420 (2002).
[18] W. Wulfhekel *et al.*, Surf. Sci. **348**, 227 (1996).
[19] P. Stoltze, J. Phys. Condens. Matter **6**, 9495 (1994).
[20] D. M. Eigler and E. K. Schweizer, Nature (London) **334**, 524 (1990).
[21] G. Meyer *et al.*, Single Molecules **1**, 79 (2000).
[22] A. J. Heinrich, C. P. Lutz, J. A. Gupta, and D. M. Eigler, Science **298**, 1381 (2002).
[23] For the row-of-adatom case our GGA-DFT (3-by-1, five-layer unit cell, 4-by-12 k points, 30 Ry cutoff) yields a 8.6 meV/atom fcc preference.
[24] $\nu_0 = 1 \times 10^{12}\ s^{-1}$ results from extensive finite-difference DFT calculations of the local fcc- and hcp-monomer dynamics as will be described in a forthcoming publication.
[25] A. Bogicevic *et al.*, Phys. Rev. Lett. **85**, 1910 (2000).
[26] P. Hyldgaard and M. Persson, J. Phys. Condens. Matter **12**, L13 (2000).
[27] K. A. Fichthorn and M. Scheffler, Phys. Rev. Lett. **84**, 5371 (2000).
[28] G. Wahnström, in *Interactions of Atoms and Molecules with Solid Surfaces*, edited by V. Bortolani, N. H. March, and M. P. Tosi (Plenum Press, New York, 1990), p. 529.
[29] L. J. Lauhon and W. Ho, Phys. Rev. Lett. **85**, 4566 (2000); **89**, 079901 (2002).
[30] D. L. Hill and J. A. Wheeler, Phys. Rev. **89**, 1102 (1953).